ISSN 1330-3651 (Print), ISSN 1848-6339 (Online)
https://doi.org/10.17559/TV-20250208002346
Original scientific paper

Maximizing Photovoltaic Power Output in Partial Shading Conditions for Electric Vehicle Applications: A Comparative Study of Intelligent Control Strategies

Nabil MCHIRGUI, Ahmed LAKHSSASSI, Habib KRAIEM*, Mohamed RAHOUTI, Hady ABDEL MAKSOUD, Nordine QUADAR

Abstract: The increasing demand for sustainable transportation has positioned Electric Vehicles (EVs) as a key application area for photovoltaic (PV) systems. This study aims to enhance PV performance under Partial Shading Conditions (PSCs) by employing advanced Maximum Power Point Tracking (MPPT) algorithms. A comprehensive simulation model featuring a boost converter and battery integration is developed to evaluate and compare three MPPT techniques: the conventional Perturb and Observe (P&O) method, Grey Wolf Optimization (GWO), and Fuzzy Logic Control. Unlike previous studies, this work conducts a structured and comparative performance analysis across four distinct and progressively complex shading scenarios. Performance metrics include average power output, convergence time, and steady-state oscillations. Simulation results under shading patterns SP1 to SP4 indicate that the Fuzzy Logic approach achieves superior performance, with mean power outputs of 997.094 W (SP1) and 410.081 W (SP4), outperforming GWO by 1.7% and 0.7%, respectively. These findings offer quantitative evidence for the effectiveness of intelligent MPPT methods in enabling robust and efficient PV integration for EV applications.

Keywords: electric vehicles (EVs); fuzzy; grey wolf optimization GWO; maximum power point tracking (MPPT); perturb and observe (P&O), photovoltaic system

1 INTRODUCTION

In recent decades, the utilization of renewable energies as an ecologically conscious substitute for fossil fuels and nuclear energy has garnered immense appeal due to their inexhaustible nature, minimal environmental impact, and adaptability to decentralized power generation [1-3]. As a result, cutting-edge technologies are actively under development to harness the potential of these energy sources.

Among the prevalent renewable options, solar energy emerges as a standout choice, serving as the foundation for photovoltaic (PV) energy generation through solar panels. The trajectory of solar energy's growth is marked by exponential progress. Notably, it operates on a decentralized premise, catering effectively to the demands of local communities and authorities, while curbing energy losses during transmission. This decentralization spurs increased utility and heightened efficiency. In stark contrast to the visual and auditory disruptions caused by wind turbines, solar energy remains silent and unobtrusive, making it a favourite choice in residential areas. The robust expansion of the solar energy market further underscores its ascendancy [4]. Photovoltaic (PV) generators find diverse applications, with isolated systems and grid-connected systems being the primary categories. The performance and efficiency of PV systems are significantly influenced by factors like radiation and temperature. Low radiation levels lead to reduced energy output, while high temperatures cause a decrease in power generation [5].

PV arrays have become indispensable for harnessing solar energy due to their ease of installation, low maintenance requirements, and cost-effectiveness. Despite the presence of electric motors powered by PV cells in the market, their reliance on carbon brushes or DC/AC converters affects their reliability and suitability for specific applications.

Amid a global emphasis on sustainable technologies, the evolution of transportation has led to the rise of electric vehicles (EVs) and their unique subset: solar vehicles [6]. EVs, propelled by electricity rather than conventional fuels, have transformed the automotive landscape by offering cleaner and more energy-efficient mobility options. However, within the realm of EVs, a fascinating niche has emerged in the form of solar vehicles, an innovation that integrates renewable energy directly into the driving experience [7]. Solar vehicles are equipped with solar panels that capture sunlight and convert it into electric power, enabling propulsion or charging of onboard batteries. This integration of solar technology holds the promise of extending the range of EVs, reducing reliance on external charging infrastructure, and enhancing the sustainability quotient of personal transportation. This exploration delves into the world of electric vehicles and the innovative concept of solar vehicles, shedding light on their mechanics, benefits, challenges, and potential contributions to a greener and more environmentally conscious future of transportation [8].

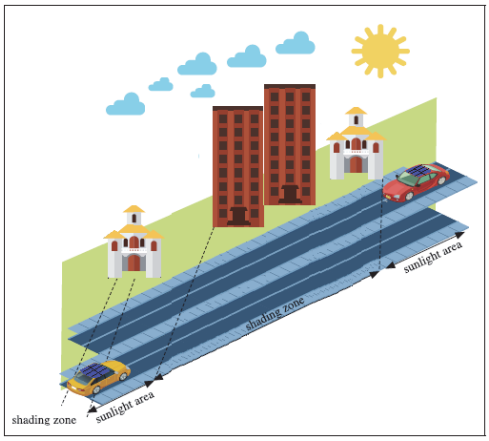

Figure 1 Example shading zone/irradiation path simulation

Fig. 1 illustrates typical partial shading conditions that solar electric vehicles (EVs) often encounter in urban environments. Shading caused by nearby buildings, trees, or other obstacles leads to non-uniform irradiance across photovoltaic (PV) modules. This irregular exposure results in complex power-voltage (*P-V*) characteristics with multiple local maxima, making it difficult for conventional MPPT algorithms to reliably track the global maximum power point. As a result, the efficient operation of PV

systems under such conditions becomes highly dependent on the effectiveness of the MPPT technique used [9].

Shading introduces two major technical challenges for PV systems [10, 11]. The first is mismatch losses, where the current output of the entire PV array is limited by the weakest (shaded) module. The second is the hot spot effect, which occurs when a shaded module absorbs power instead of producing it, potentially causing localized overheating and long-term damage. These issues substantially degrade system performance and pose reliability and safety risks, especially in mobile solar-powered applications like EVs [12, 13].

To overcome these limitations, researchers have proposed various intelligent MPPT algorithms capable of adapting to rapidly changing environmental conditions [14], for instance, compared P&O, Fuzzy Logic, and ANFIS-based controllers, demonstrating improved tracking performance with intelligent techniques, though steady-state dynamics were not examined. Priyadarshi et al. [15] developed a TS-fuzzy RBF neural network that provided better adaptability but required complex model tuning. Mirjalili et al. [16] introduced the Grey Wolf Optimization (GWO) algorithm, which has been applied successfully to MPPT problems, yet its transient behavior under diverse shading conditions remains underexplored. More recently, Ali et al. [17] proposed an Adaptive Fuzzy Logic Controller with grid integration, but without evaluating its convergence behavior across multiple shading patterns.

While these contributions are valuable, most studies emphasize tracking accuracy in isolation and often overlook other critical performance aspects such as convergence time, dynamic response, and robustness under varying PSC scenarios. In contrast, the present work offers a comprehensive comparison of three MPPT strategies P&O, GWO, and Fuzzy Logic evaluated under four distinct and progressively complex shading conditions. By jointly analyzing mean power output, convergence speed, and steady-state oscillations, this study aims to deliver practical insights for designing reliable PV systems tailored for EV integration.

To conduct this analysis, a complete simulation framework is developed using MATLAB/Simulink. The framework incorporates a PV array, a boost converter, and a lithium-ion battery model. Each MPPT method is tested under identical conditions and evaluated based on multiple performance metrics. The results serve to highlight the relative strengths and limitations of each technique, particularly in challenging partial shading scenarios.

To conclude, the key original contributions of this study are summarized as follows:

1. A structured comparative analysis of three MPPT techniques Perturb and Observe (P&O), Grey Wolf Optimization (GWO), and Fuzzy Logic under four distinct partial shading scenarios designed to reflect realistic urban environments.
2. A detailed performance evaluation that goes beyond traditional MPP tracking accuracy by including mean power output, convergence time, and steady-state oscillations key parameters for practical deployment in solar-powered EVs.
3. Identification of trade-offs between response speed and tracking stability, offering insights into selecting and tuning intelligent controllers based on application-specific needs.
4. A full-system simulation in MATLAB/Simulink that includes realistic PV, converter, and battery models, providing a reproducible experimental platform for future research and validation.

Following this introduction, the paper is organized as follows: Section 2 presents the architecture of the electric vehicle system. Section 3 describes the modeling of the PV array, boost converter, and battery. Section 4 details the MPPT control strategies (P&O, Fuzzy, and GWO). Section 5 discusses simulation results and comparative analysis. Finally, Section 6 summarizes the key findings and outlines directions for future research.

2 THE ELECTRIC VEHICLE ARCHITECTURE

Electric vehicles (EVs) encompass a range of propulsion technologies, including Battery Electric Vehicles (BEVs), Plug-in Hybrid Electric Vehicles (PHEVs), and Hybrids [18, 19]. These vehicles typically feature a central battery pack that directly powers an electric motor driving the wheels [20]. BEVs offer numerous advantages such as zero emissions, simplified drive train designs, energy efficiency, and long-term cost savings. However, challenges like limited range and charging infrastructure persist. Ongoing advancements in battery technology are extending BEV ranges and reducing charging times, playing a crucial role in achieving emission-free transportation [21]. This progress underscores the importance of advancing battery technology, expanding charging infrastructure, and addressing sustainability considerations for a transformative shift towards sustainable mobility.

A solar-powered electric vehicle, as illustrated in the Fig. 2, further enhances the concept of sustainable mobility. It integrates a solar panel to harness renewable energy, a multiport power converter to manage energy distribution, a battery for energy storage, and an electric motor controlled by a motor driver for propulsion. This design not only optimizes energy efficiency but also minimizes reliance on conventional charging infrastructure, making it a promising solution for sustainable transportation. According to the findings presented in [22], a study on the well-to-wheel energy efficiency of different powertrain technologies highlights the superior performance of electric vehicles (EVs) compared to internal combustion engine (ICE) vehicles. The study shows that EVs, such as the Nissan Leaf, consume an average of 0.470 MJ/km, while ICE vehicles consume approximately 2.456 MJ/km, underscoring the significant energy efficiency advantage of EVs. This well-to-wheel analysis considers the entire energy chain, including extraction, transformation, transport, and energy use. However, it does not factor in "gray energy", which refers to the energy required for manufacturing and recycling vehicle components. Due to the complexity of battery production, EVs are likely to have higher "gray energy" demands compared to ICE vehicles.

Battery Electric Vehicles (BEVs) offer the major advantage of zero emissions and have significantly improved in range and charging efficiency. Modern BEVs now achieve ranges of 300-500 kilometers per charge,

making them practical for long-distance travel and not just city commutes. Fast-charging technologies further reduce charging times, enhancing user convenience. The integration of solar-powered systems in EVs adds to their energy efficiency, reducing reliance on external charging while promoting environmental sustainability. These advancements address earlier limitations, demonstrating the growing practicality and appeal of BEVs for a wider range of transportation needs.

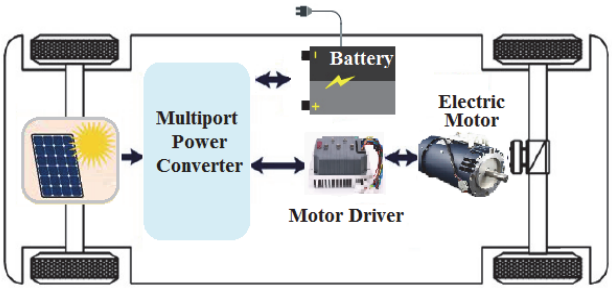

Figure 2 Battery electric vehicle architectures

3 PV SYSTEM MODEL

This section presents the modeling of the photovoltaic (PV) system, including its key components and operational principles. The system consists of a PV array exposed to varying sunlight conditions, a DC-DC boost converter for voltage regulation [23], and Maximum Power Point Tracking (MPPT) algorithms to optimize energy extraction. The Fig. 3 illustrates the integration of these components, highlighting how the MPPT controller dynamically adjusts the converter's duty cycle to ensure the PV array operates at its maximum power point, even under partial shading. This model serves as the foundation for evaluating the performance of different MPPT techniques.

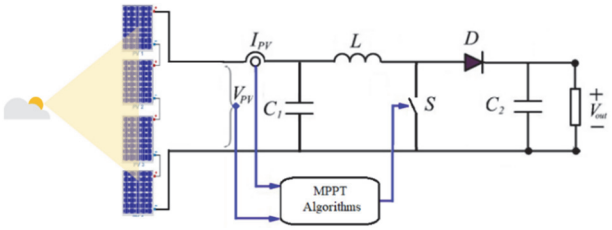

Figure 3 Diagram of the Photovoltaic System with MPPT Algorithm Integration

3.1 Photovoltaic Cell Model

A photovoltaic module is composed of multiple solar cells arranged in series and parallel configurations to produce the required voltage and current levels. Each solar cell operates as a p-n junction semiconductor that generates direct current when exposed to sunlight. For analysis, this study utilizes the single-diode model illustrated in Fig. 4. This model strikes an effective balance between simplicity and accuracy, providing a fundamental yet precise representation of the PV system's behavior [24].

The equivalent circuit of the generalized model comprises a photocurrent source (I_{ph}), a diode, a parallel resistance (R_p) representing leakage currents, and a series resistance (R_s) accounting for the electrical losses caused by the contact interfaces between the semiconductor material and the metal components.

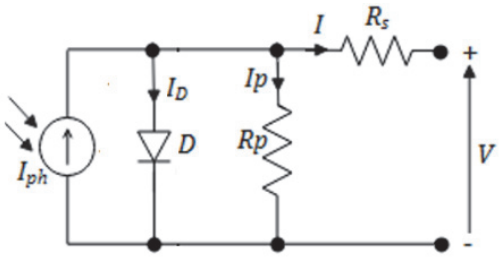

Figure 4 Simplified equivalent circuit of solar cell

The current I can be determined by applying Kirchhoff's law in Fig. 4:

$$I = I_{ph} - I_D - I_p \tag{1}$$

I_{ph} the photo current and I_p represents the current passing through the R_p can be determined as:

$$I_p = \frac{V + R_S I}{R_p} \tag{2}$$

I_D denotes the diode current (related to the saturation current). This is given by the following equation [25]:

$$I_D = I_{sd}\left(\exp\left(\frac{q\cdot(V + R_S\cdot I)}{n\cdot \mathrm{K}\cdot T}\right) - 1\right) \tag{3}$$

where I_{sd} denotes the reverse saturation current, q the charge of electron (1.602×10^{-19} C), K the constant of Boltzmann (1.38×10^{-23} J/K), T the temperature of cell in Kelvin (K) and finally n is the ideal factor.

We replace in Eq. (1):

$$I = I_{ph} - I_{sd}\left(\exp\left(\frac{q\cdot(V + R_S\cdot I)}{n\cdot \mathrm{K}\cdot T}\right) - 1\right) - \frac{V + R_S I}{R_p} \tag{4}$$

A single PV cell typically generates less than 2 W of power at approximately 0.5 V. Therefore, multiple cells must be connected in series and parallel within a module to achieve the required power output [26]. A photovoltaic array consists of multiple PV modules electrically interconnected in series N_s and parallel N_p configurations to produce the desired voltage and current levels.

The V-I relationship for a photovoltaic (PV) module is expressed through the following characteristic equation:

$$I = N_p\cdot I_{ph} - N_p\cdot I_{sd}\left[\exp\left(\frac{q\left(\frac{V}{N_S} + \frac{I\cdot R_S}{N_p}\right)}{\mathrm{K}\cdot T\cdot n}\right) - 1\right] - \frac{\left(\frac{N_p\cdot V}{N_S} + I\cdot R_S\right)}{R_p} \tag{5}$$

The specifications of the PV module utilized in this study are provided in Tab. 2.

3.2 Boost Converter

DC/DC converters are crucial in power systems for regulating and adapting voltage levels to meet specific application requirements, ensuring efficiency and stability. Among these, the boost converter is particularly popular in photovoltaic (PV) systems due to its ability to step up the low and fluctuating voltage from solar panels to the required levels for loads or storage systems [27]. This is essential in scenarios like partial shading or variable sunlight. Additionally, in Maximum Power Point Tracking (MPPT) applications, the boost converter is highly efficient, simple to implement, and capable of operating across a wide range of input voltages. It enables the MPPT controller to dynamically adjust the operating point of the PV system, ensuring maximum power extraction and making it an ideal choice for modern solar energy solutions. To derive the modeling equations for the Boost Converter shown in the figure, we analyze the system for the two states of operation: when the switch (S) is ON and OFF.

Steady-State Voltage Conversion Ratio: For steady-state operation, the energy stored in L during the ON phase equals the energy released during the OFF phase. The output-to-input voltage ratio is:

$$V_{out} = \frac{V_{PV}}{1-D} \tag{6}$$

where D is the duty cycle

State-Space Representation: Using the state variables: $x_1 = i_L$: inductor current; $x_2 = V_{C2} = V_{out}$: capacitor C_2 voltage.

The state-space equations are:

- When S is ON:

$$\dot{x}_1 = \frac{V_{PV}}{L_1}, \dot{x}_2 = -\frac{x_2}{R \cdot C_2} \tag{7}$$

- When S is OFF:

$$\dot{x}_1 = \frac{V_{PV} - x_2}{L_1}, \dot{x}_2 = \frac{x_1}{C_2} - \frac{x_2}{R \cdot C_2} \tag{8}$$

The above equations describe the dynamic behavior of the converter. These models can be used to design controllers, simulate transient responses, and optimize performance under varying PV conditions.

3.3 Battery Model

Batteries play a vital role in electric vehicles (EVs), with their performance influenced by numerous factors. To evaluate and predict battery behavior, various mathematical models have been developed, including the Rint model, RC model, Thevenin model, and PNGV model, alongside electrochemical approaches such as the Shepherd model, Unnewehr universal model, Nernst model, and combined model. These models are extensively utilized in EV research to study battery polarization characteristics. Notably, the Thevenin model and advanced alternatives like the improved NPV model have proven particularly effective in accurately representing the performance of lithium-ion batteries [28].

The schematic diagram of the new NPV model is illustrated in Fig. 5. This model represents the open-circuit voltage (V_{oc}) as a function of the state of charge (SoC). In this model, K_0, K_1 and K_2 are constants selected to ensure the model accurately fits the experimental data. R_0 represents the ohmic resistance, while R_p denotes the polarization resistance. C_p is the polarization capacitance, used to characterize the transient response during the processes of charging and discharging, with V_p representing the voltage across C_p. The electrical characteristics of the model are represented by the following equation:

$$\begin{cases} V_t = V_{oc} - V_p - I_L R_o \\ \dot{V}_p = \dfrac{I_L}{C_p} - \dfrac{V_p}{C_p R_p} \\ V_{oc} = \mathrm{K}_0 + \mathrm{K}_1 \ln SoC + \mathrm{K}_2 \ln\left(1 - SoC\right) \end{cases} \tag{9}$$

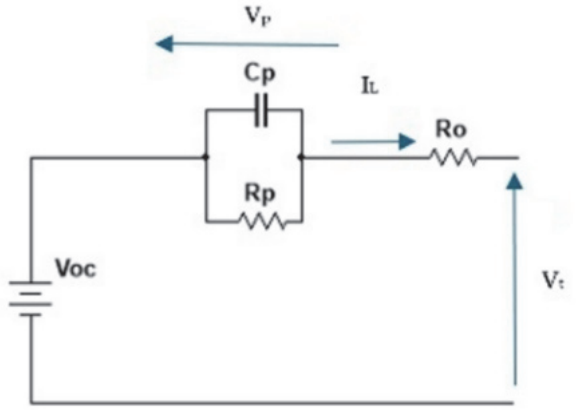

Figure 5 Schematic diagram for the new electrochemical-polarization model

The Fig. 5 depicts an equivalent circuit model of the battery, illustrating its internal dynamics. The open-circuit voltage (V_{oc}) is the primary energy source, while R_0, the internal resistance, represents energy losses. The parallel combination of R_p and C_p models the transient polarization effects, with I_L and V_t indicating the load current and terminal voltage, respectively. This model provides a detailed representation of the battery's charging and discharging behavior, enhancing the accuracy of performance prediction and control in EV applications.

4 MPPT TECHNIQUES FOR PHOTOVOLTAIC SYSTEMS

Photovoltaic (PV) systems face challenges due to variable solar irradiance, making consistent maximum energy production difficult. To address this, Maximum Power Point Tracking (MPPT) dynamically adjusts system output for efficient operation under changing conditions. MPPT operates by monitoring and adjusting the voltage output from a boost converter to match the battery's requirements, maximizing power transfer.

The Perturb and Observe (P&O) technique is a widely used MPPT method due to its simplicity but struggles with efficiency under rapidly changing conditions. Advanced algorithms like fuzzy control and Grey Wolf Optimization

(GWO) improve tracking accuracy and adaptability, offering enhanced performance in dynamic environments.

4.1 Perturb and Observe

The Perturb and Observe algorithm is among the most commonly employed methods for MPPT in photovoltaic PV systems [29]. Its simplicity, ease of implementation, and cost-effectiveness make it a preferred choice for maximizing the energy harvested from solar panels. The P&O method operates by iteratively adjusting the operating point of the PV system and observing the effect on power output to identify the Maximum Power Point (MPP).

Basic Principle:

- The P&O algorithm perturbs (changes) the voltage or current of the PV system and observes the resulting change in power output.
- The direction of perturbation is adjusted based on whether the power output increases or decreases.

a) Steps of Operation:

- Increase in Power *($\Delta P > 0$):* If a perturbation in voltage (ΔV) results in an increase in power ($\Delta P > 0$), the operating point is moving closer to the MPP. The algorithm continues perturbing in the same direction.
- Decrease in Power *($\Delta P < 0$):* If a perturbation in voltage results in a decrease in power ($\Delta P < 0$), the operating point is moving away from the MPP. The algorithm reverses the direction of perturbation.

b) Iterative Process:

- This process repeats continuously until the operating point converges at the MPP, where maximum power is extracted from the PV system.
- The principles of this algorithm are illustrated through a flowchart, as shown in Fig. 6.

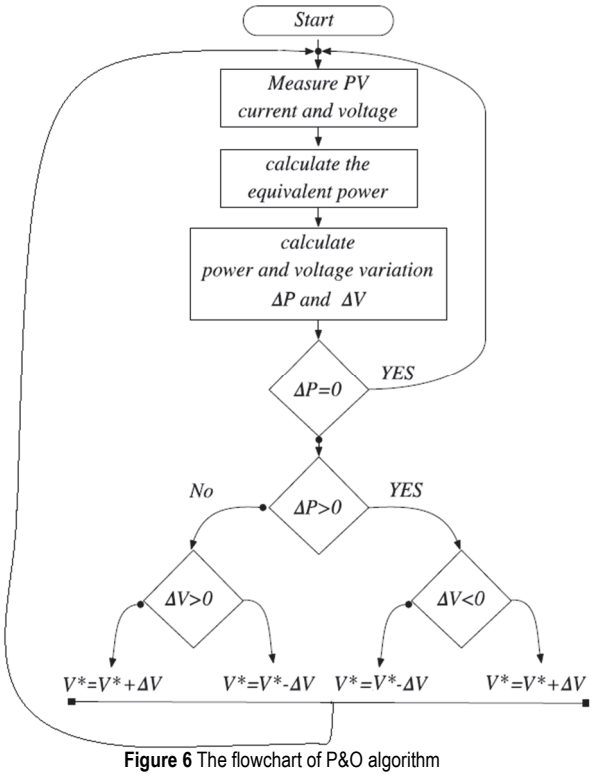

Figure 6 The flowchart of P&O algorithm

The Perturb and Observe (P&O) MPPT technique is a robust, simple, and cost-effective method for optimizing the power output of PV systems. While it is highly suitable for systems operating under stable conditions, its limitations in dynamic or shaded environments must be considered. With proper tuning and application, P&O remains one of the most practical solutions for MPPT in photovoltaic systems.

4.2 The Fuzzy MPPT Controller

With the advancements in microcontrollers, fuzzy logic control has gained popularity [30]. This technique offers several advantages, including its ability to handle imprecise input values and its independence from high-precision mathematical models. Furthermore, it can effectively deal with non-linearities. The principle of a fuzzy command involves two input variables: the error (E) and the rate of error change (ΔE), along with an output variable $\Delta\alpha$ (change in duty cycle). The determination of the output variable, which drives the static converter to achieve the desired PPM (Pulse Position Modulation), is based on a truth table and the evolution of the input parameters.

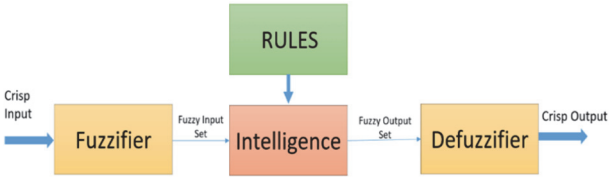

Figure 7 Fuzzy logic architecture

In the literature, fuzzy logic control typically involves three steps: fuzzification, fuzzy rule algorithm, and defuzzification, as depicted in the Fig. 7. During fuzzification, the digital input variables are transformed into linguistic variables, which provide a more intuitive representation of the data for use in fuzzy logic systems. These linguistic variables can take one of five possible values: Negative Big (NB), Negative Small (NS), Zero (ZE), Positive Small (PS), and Positive Big (PB). This categorization allows the fuzzy system to interpret and process numerical inputs in a way that mimics human reasoning, enabling effective decision-making in complex systems. The Fig. 8 illustrates the membership functions corresponding to these linguistic variables, showing how input values are mapped to their respective categories over the range of −1 to 1, where each curve represents a specific linguistic term.

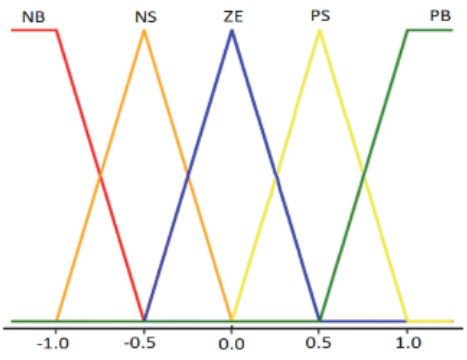

Figure 8 Membership functions for error

The input parameters E and ΔE are linked to the following equations:

$$E(k)=\frac{P(k)-P(k-1)}{V_{pv}(k)-V_{pv}(k-1)} \tag{10}$$

$$\Delta E(k)=E(k)-E(k-1) \tag{11}$$

According to the evolution of the input parameters and respecting a truth Tab. 1, a value will be assigned to the output parameter $\Delta\alpha$.

The linguistic variable $\Delta\alpha$ is determined based on various combinations of E and ΔE. For instance, when the input variables (E and ΔE) are assigned values PB and ZE, indicating operation far from the PPM, the truth table assigns the value PB to the output variable $\Delta\alpha$. This implies a strong positive variation of the duty cycle to achieve the PPM.

Table 1 Fuzzy logic controller truth table

ΔE / E	NB	NS	ZE	PS	PB
NB	ZE	ZE	NB	NB	NB
NS	ZE	ZE	NS	NS	NS
ZE	NS	ZE	ZE	ZE	PS
PS	PS	PS	PS	ZE	ZE
PB	PB	PB	PB	ZE	ZE

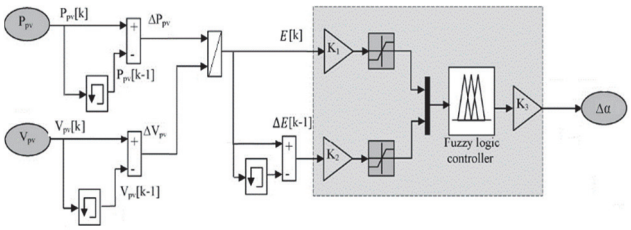

Figure 9 Takagi-Sugeno (TKS) fuzzy inference model

This Fig. 9 illustrates the fuzzy logic controller (FLC) used for Maximum Power Point Tracking (MPPT) in photovoltaic systems. It demonstrates how the FLC processes the error E[k] and the change in error ΔE[k] derived from the power P_{pv} and voltage V_{pv} of the photovoltaic panel to correct the $\Delta\alpha$ of the converter, ensuring optimal power extraction. The constants K_1, K_2 and K_3 are the adaptive gains that require online adjustment.

The flowchart (Fig. 10) illustrates the fuzzy logic-based MPPT algorithm designed to optimize photovoltaic system performance. The fuzzy inference model employed in this system is the Takagi-Sugeno model. During the defuzzification phase, the center of gravity position of the resulting membership function is calculated, and its abscissa serves as the regulator's output. As previously described, the FLC optimizes the reference voltage by strategically selecting the variation of the duty ratio $\Delta\alpha$ to track the maximum power. This process involves initializing the duty ratio (D), measuring voltage and current values, calculating power, and determining the error (E) and its change (ΔE). The fuzzy logic controller then processes these inputs through fuzzification, rule-based inference, and defuzzification to adjust the duty ratio for achieving maximum power point tracking (MPPT).

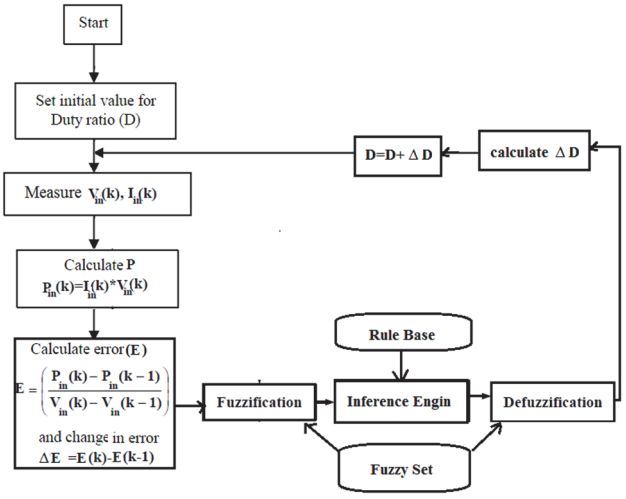

Figure10 Fuzzy logic-based MPPT algorithm flowchart

4.3 GWO MPPT Controller

In 2014, Mirjalili, introduced the GWO method as a novel metaheuristic optimization algorithm [16]. This algorithm aims to find the best solution to a problem by simulating the social hierarchy of grey wolves and analyzing the behavior of the victim. During the hunting operation, the GWO algorithm emulates the hierarchical dominance observed in real grey wolf groups until their movements converge. The hierarchical commands within the group can be categorized into four types, as depicted in Fig. 10. At the top level of social dominance is the alpha (α), responsible for making decisions related to hunting and leading the other wolves in the pack. The alpha group is considered the best solution. The second level in the chain of command is called Beta, where wolves monitor the actions of other groups and assist the alpha in decision-making. In the absence of alphas due to death or aging, betas can assume their role.

The lower ranks consist of Omega and Delta, with the latter being the lowest and last to eat after the Alpha and Beta wolf groups. In wolf packs, the hunting process involves three primary steps: chasing, surrounding, and attacking.

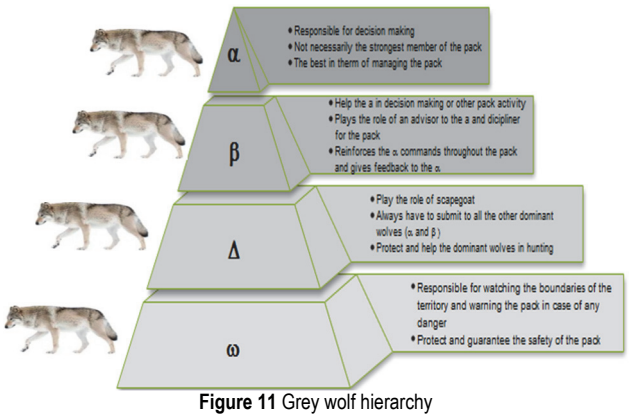

Figure 11 Grey wolf hierarchy

Grey wolves are randomly assigned positions according to an algorithm that starts with a fixed number of grey wolves.

The following equations explain how each group of the pack encircles the prey:

$$D = \left| C \cdot X_p(t) - X(t) \right| \tag{12}$$

$$X(t+1) = \left| X_p(t) - A \cdot D \right| \tag{13}$$

$X(t)$ is the grey wolf vector position, $X_p(t)$ is the position vector of prey

The vectors A and C can be expressed by the following equations:

$$\begin{cases} \vec{A} = 2 \cdot \vec{a} \cdot \vec{r}_1 - \vec{a} \\ \vec{C} = 2 \cdot \vec{r}_2 \end{cases} \text{ with: } a = 2 \cdot \left(1 - \frac{t}{T_{\max}} \right) \tag{14}$$

$T_{\max}$, t: the iterations total number and the current iteration, r_1 , r_2: randomly chosen in the interval [0, 1].

The term $X_p(t + 1)$ refers to the update of the prey position determined from the positions of gray wolves groups α, β, and Δ. The following mean function is employed to achieve this objective [16]:

$$\vec{X}_p(t+1) = \frac{\vec{X}_1(t) + \vec{X}_2(t) + \vec{X}_3(t)}{3} \tag{15}$$

where:

$$\begin{aligned} \vec{D}_\alpha &= \left| \vec{C}_1 \vec{X}_\alpha(t) - \vec{X}(t) \right| \\ \vec{D}_\beta &= \left| \vec{C}_2 \vec{X}_\beta(t) - \vec{X}(t) \right| \\ \vec{D}_\Delta &= \left| \vec{C}_3 \vec{X}_\Delta(t0) - \vec{X}(t) \right| \end{aligned} \tag{16}$$

and:

$$\begin{aligned} \vec{X}_1(t) &= \vec{X}_\alpha(t) - \vec{A}_1 \cdot \vec{D}_\alpha \\ \vec{X}_2(t) &= \vec{X}_\beta(t) - \vec{A}_2 \cdot \vec{D}_\beta \\ \vec{X}_3(t) &= \vec{X}_\Delta(t) - \vec{A}_3 \cdot \vec{D}_\Delta \end{aligned} \tag{17}$$

Eq. (12) represents the distance from the current position, aiming to minimize it to bring the subsequent position denoted by Eq. (13) closer to the position of the victim, which signifies the correct solution of the problem $X_P(t)$.

The parameter "a" in this algorithm linearly decreases from 2 to 0 during successive iterations using Eq. (14), effectively modeling the wolves' behavior when approaching the victim during the exploration phase. If the condition $|A| < 1$ is met in this phase, the wolves initiate an attack on the victim.

The alpha group, recognized as the leaders, holds the most accurate knowledge of the prey's location. Upon identifying the prey's position, the hunt is primarily led by the alpha group, with occasional contributions from the beta and delta groups. Meanwhile, the rest of the pack prioritizes attending to injured wolves and ensuring the well-being of the group. Once the prey ceases movement, the wolves initiate their attack, bringing the hunt to an end.

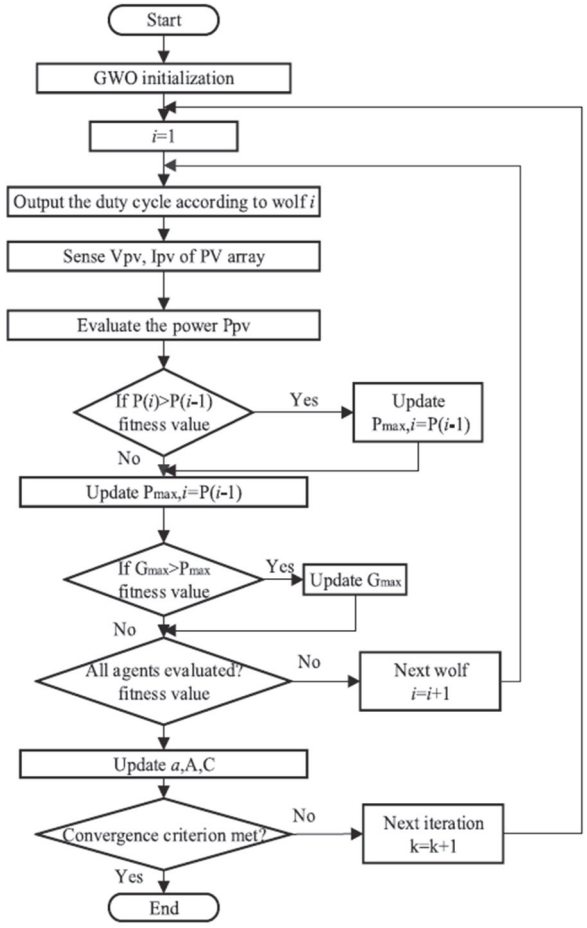

Figure 12 Flowchart of GWO-based MPPT algorithm for PV systems

The flowchart shown in the Fig. 12 illustrates the GWO-based MPPT algorithm for photovoltaic systems. It initializes parameters, evaluates power (P_{pv}) for each agent (wolf), updates fitness values, and identifies the global maximum power ($G_{\max}$). The process iterates, adjusting parameters, until the convergence criterion is satisfied, ensuring optimal power point tracking.

5 RESULTS AND DISCUSSION

To study the comparative performance of the P&O, GWO, and Fuzzy MPPT control methods, a small prototype system was implemented. The prototype consists of four API-P250V photovoltaic modules connected in series. These modules are tested under various levels of shading conditions, as detailed in Tab. 3. The modules are connected to a DC boost converter, which is controlled by the output of the MPPT controller algorithm. The system configuration is illustrated in Fig. 3.

The entire system, including the photovoltaic modules, boost converter, and MPPT controller, is simulated using MATLAB/SIMULINK 2021. This setup enables a thorough evaluation of the effectiveness and feasibility of the three MPPT techniques under different shading scenarios, facilitating a comprehensive comparison of their performance.

The specifications of the photovoltaic module are listed in Tab. 2.

Table 2 Table API-P250V module specifications at STC

Characteristics	Value
P_{mpp}	250 .536 W
V_{mpp}	31.2 V
I_{mpp}	8.03 A
I_{sc}	8.52 A
I_{oc}	37.2 V
Current temperature coefficient	0.057582 A/°C
Voltage temperature coefficient	−0.3342 V/°C
No. of cells	60

Tab. 3 illustrates the different shading patterns (SPs) applied to the photovoltaic (PV) sub-modules in the system, with each shading pattern characterized by varying levels of solar insolation (measured in W/m²) on the four sub-modules (Gpv11, Gpv12, Gpv21, and Gpv22).

- SP1: All sub-modules receive uniform insolation of 1000 W/m², representing standard non-shaded conditions.
- SP2: Sub-module Gpv11 is shaded, receiving only 300 W/m², while the other three sub-modules (Gpv12, Gpv21, and Gpv22) maintain full insolation of 1000 W/m².
- SP3: Both Gpv11 and Gpv12 are shaded, with insolation levels of 300 W/m² and 500 W/m², respectively, while Gpv21 and Gpv22 remain fully illuminated at 1000 W/m².
- SP4: A more complex shading scenario is represented, where Gpv11 and Gpv12 receive 300 W/m² and 500 W/m², respectively, Gpv21 receives reduced insolation of 800 W/m², and only Gpv22 remains fully illuminated at 1000 W/m².

These various partial shading conditions are essential for evaluating and comparing the performance of MPPT algorithms in maintaining efficient power output.

Table 3 The four shading patterns used in this study

Pattern no.	Insolation on PV sub-modules / W/m²			
	Gpv11	Gpv12	Gpv21	Gpv22
SP1	1000	1000	1000	1000
SP2	300	1000	1000	1000
SP3	300	500	1000	1000
SP4	300	500	800	1000

The Fig. 13 illustrates the power-voltage (P-V) characteristics of a photovoltaic system under different shading patterns (SP1 to SP4), showing that under shading conditions, the P-V curves exhibit multiple local maxima. This highlights the critical importance of employing advanced MPPT algorithms to ensure optimal power extraction by accurately identifying and tracking the global maximum point of the curves.

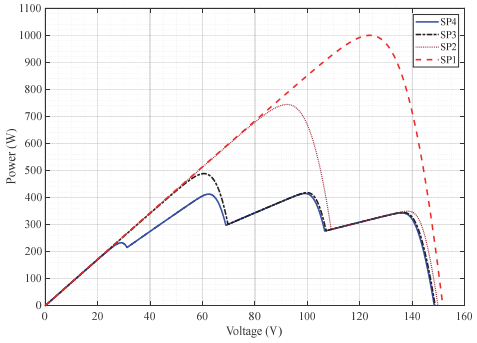

Figure 13 Analysis of PV characteristics for different types of shading

The Tab. 4 presents the optimal values of maximum power (P_{mpp}), voltage (V_{mpp}), and current (I_{mpp}) corresponding to the different shading patterns (SP1 to SP4) as derived from the P-V characteristics in the Fig. 13.

These results represent the global maxima that advanced MPPT controllers must achieve to ensure efficient and optimal power extraction from the photovoltaic system under varying shading conditions.

Fig. 14 illustrates the results of the SP1 shading pattern for three MPPT control techniques: P&O, GWO, and Fuzzy. The plots show the PV voltage, duty cycle, PV current, and PV power over time. The GWO and Fuzzy methods demonstrate improved tracking performance, achieving faster convergence to the maximum power point (MPP). However, both GWO and Fuzzy methods exhibit noticeable oscillations during steady-state operation, while the P&O method provides a more stable, albeit slower, response. These oscillations highlight the trade-off between dynamic response and stability in advanced MPPT techniques.

Table 4 Analysis of PV characteristics under varying shading patterns

	P_{mpp} / W	V_{mpp} / V	I_{mpp} / A
PS1	999.351	123.816	8.071
PS2	743.822	92.19	8.068
PS3	488.311	60.56	8.063
PS4	412.559	62.386	6.613

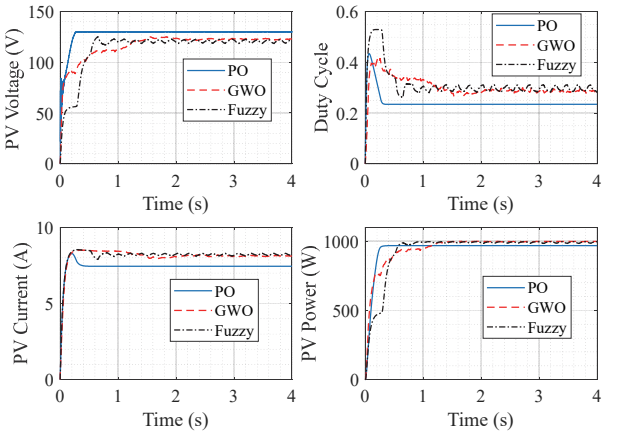

Figure 14 Performance comparison of P&O, GWO, and Fuzzy MPPT techniques under SP1 shading condition

Notably, the PV power results from all the MPPT controllers achieve the optimal value, approximately 999.351 W, as expected in this shading condition. This is because SP1 presents a single global maximum, ensuring no ambiguity in power tracking for any of the controllers.

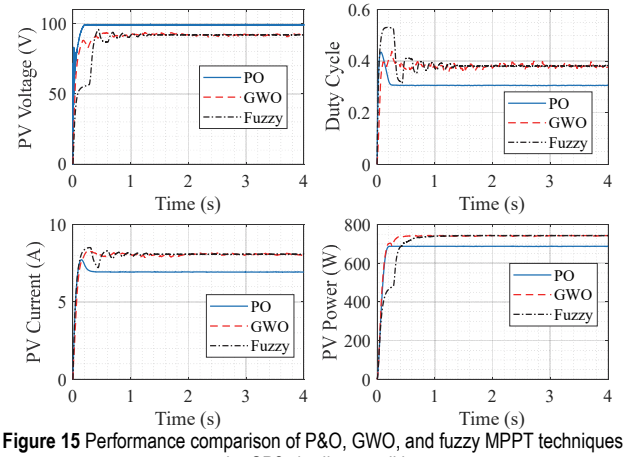

Figure 15 Performance comparison of P&O, GWO, and fuzzy MPPT techniques under SP2 shading condition

Fig. 15 illustrates the performance of the MPPT control techniques P&O, GWO, and Fuzzy under shading pattern SP2. The plots display PV voltage, current, duty cycle, and power over time. Notably, the P&O method struggles to track the global maximum power due to its inability to distinguish between local and global maxima under partial shading conditions. Conversely, both GWO and Fuzzy MPPT algorithms effectively achieve the maximum power. The Fuzzy MPPT shows slower convergence compared to GWO but exhibits minimal oscillations, ensuring steady and reliable performance. These results emphasize the superior tracking capability of intelligent MPPT techniques like GWO and Fuzzy under complex shading scenarios.

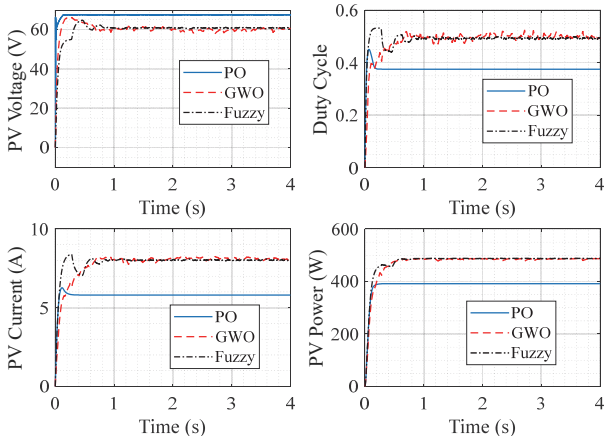

Figure 16 Performance comparison of P&O, GWO, and fuzzy MPPT techniques under SP3 shading condition

Under shading pattern SP3, which features three local maxima in the power-voltage curve (Fig. 13), Fig. 16 compares the performance of MPPT control techniques P&O, GWO, and Fuzzy. The P&O method struggles to accurately track the global maximum power due to its inability to distinguish between local and global maxima, resulting in suboptimal power extraction. In contrast, the Fuzzy MPPT smoothly outperforms GWO, offering faster convergence, minimal oscillations, and negligible steady-state error.

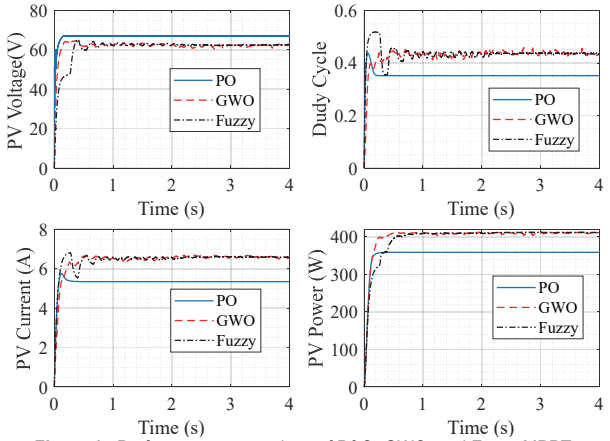

Figure 17 Performance comparison of P&O, GWO, and Fuzzy MPPT techniques under SP4 shading condition

Under shading pattern SP4, characterized by four local maxima in the power-voltage curve, Fig. 17 demonstrates the performance of the MPPT techniques P&O, GWO, and Fuzzy. The P&O method continues to face challenges in reaching the global maximum power due to its inability to distinguish between local and global maxima, leading to suboptimal power extraction. In contrast, both Fuzzy and GWO methods successfully track the global maximum power. The GWO algorithm achieves a faster response but exhibits oscillations during convergence, while the Fuzzy MPPT method provides smoother and more precise tracking with minimal oscillations, albeit with a slower convergence rate compared to GWO.

Tab. 5 provides a comparative overview of the three MPPT algorithms - Fuzzy Logic, Grey Wolf Optimization (GWO), and Perturb and Observe (P&O) - under four distinct partial shading patterns (SP1 to SP4). The performance metrics considered include mean power output, time to reach the maximum power point (MPP), and the theoretical optimal power for each scenario.

Table 5 Comparison between the GWO and fuzzy-based MPPT methods under different partial shading patterns

Pattern no.	Tracking algorithm	Mean power / W	Time to reach MPP / s	Optimal power / W
SP1	Fuzzy	997.094	1.09826	999.351
	GWO	995.399	1.42768	
	PO	968.202	0.507843	
SP2	Fuzzy	740.284	1.04452	743.822
	GWO	739.321	0.485227	
	PO	687.776	0.258164	
SP3	Fuzzy	487.335	0.926832	488.311
	GWO	485.181	1.03577	
	PO	391.287	0.309546	
SP4	Fuzzy	410.081	1.01035	412.559
	GWO	407.054	0.44479	
	PO	358.242	0.309484	

SP1 (Uniform Irradiance)

All three algorithms perform well under SP1, which presents a single global peak and no ambiguity in power tracking. The Fuzzy MPPT achieves the highest mean power output (997.094 W), closely followed by GWO (995.399 W). The P&O method, while faster to converge (0.5078 s), yields a noticeably lower mean power (968.202 W), indicating small oscillations or deviations near the MPP. This suggests that while P&O is efficient in straightforward conditions, it compromises precision compared to intelligent methods.

SP2 (One Module Shaded)

Under moderate shading, the performance gap becomes more pronounced. Both Fuzzy and GWO successfully locate the global MPP, with Fuzzy again delivering the highest mean power (740.284 W). GWO, though slightly less accurate (739.321 W), shows superior responsiveness with the fastest convergence (0.4852 s). The P&O method achieves only 687.776 W, illustrating its tendency to lock onto local maxima in the presence of shading-induced *P-V* irregularities.

SP3 (Two Modules Shaded)

Increased shading complexity further tests algorithm robustness. Fuzzy logic continues to outperform (487.335 W) and demonstrates low oscillations and good steady-state behavior. GWO follows closely (485.181 W), albeit with a longer convergence time. P&O again falls short (391.287 W), reinforcing its inadequacy under multi-peak conditions. These results confirm that intelligent algorithms are not only more accurate but also more reliable in dynamic environments.

SP4 (Three Modules Shaded)

This represents the most complex and asymmetrical shading case. Fuzzy MPPT maintains the highest mean power (410.081 W) and precise tracking with minimal overshoot. GWO trails slightly (407.054 W) but converges more rapidly (0.4448 s), which may benefit time-critical applications. P&O continues to underperform (358.242 W), reaffirming its unsuitability for high-complexity scenarios.

5.1 Comparative Insights and Trade-offs

A key takeaway from this comparative study is the trade-off between convergence speed and tracking accuracy. GWO consistently achieves faster convergence than Fuzzy, but often at the cost of minor oscillations around the MPP. In contrast, the Fuzzy controller exhibits slightly slower response times but delivers smoother, more accurate steady-state power.

Furthermore, P&O's limitations are clearly exposed as shading complexity increases. While suitable for simple or stable conditions, its susceptibility to local extrema and lack of adaptability makes it unreliable under real-world partial shading scenarios. This underscores the need for intelligent, adaptive MPPT techniques in applications such as solar-powered EVs where irradiance conditions are inherently dynamic.

5.2 Practical Implications

For EV-integrated PV systems, where energy harvesting efficiency directly impacts battery autonomy and vehicle range, the choice of MPPT algorithm is critical. The Fuzzy MPPT offers the best balance between performance and stability, making it ideal for high-reliability systems. GWO may be preferred when faster dynamic adaptation is needed, such as in intermittently shaded routes. P&O, though computationally lightweight, is not recommended unless environmental conditions are highly predictable.

6 CONCLUSION

This study investigated and comparatively evaluated three Maximum Power Point Tracking (MPPT) techniques - Perturb and Observe (P&O), Grey Wolf Optimization (GWO), and Fuzzy Logic Control - under varying partial shading conditions. Through detailed MATLAB/Simulink simulations across four distinct shading scenarios, the research demonstrated that traditional P&O methods are limited in their ability to consistently track the global maximum power point, especially in the presence of multiple local maxima. In contrast, the fuzzy logic-based MPPT algorithm consistently delivered the highest mean power output with minimal oscillations, while the GWO algorithm provided faster convergence times with slightly lower tracking precision. By jointly analyzing mean power, convergence time, and dynamic stability, the study provides actionable insights into selecting and tuning MPPT strategies for solar-powered electric vehicle (EV) applications. These findings contribute to improving the energy efficiency, reliability, and adaptability of PV systems in real-world, dynamically shaded environments.

Future work should focus on the practical implementation of these intelligent MPPT techniques in embedded systems. In particular, deploying fuzzy logic and GWO algorithms on hardware platforms such as FPGAs or DSPs can help validate their performance under real-time constraints. Additional research is also encouraged to optimize controller parameters using adaptive or hybrid AI approaches, integrate weather prediction data, and assess long-term operational reliability under varying climatic conditions. Such developments would further enhance the deployment readiness of intelligent MPPT systems for next-generation EVs and off-grid solar applications.

Acknowledgements

The authors would like to acknowledge the support of the Université du Québec en Outaouais (UQO) and the Laboratoire d'Ingénierie des Microsystèmes Avancés (LIMA). The authors extend their appreciation to the Deanship of Scientific Research at Northern Border University, Arar, KSA for funding this research work through the project number NBU-FFR-2025-2484-14.

7 REFERENCES

[1] Gao, J., Tian, S., Yuan, C., Ma, Z., Gao, C., Yan, G., & Zhang, L. (2024). Design and optimization of a novel double-layer Helmholtz coil for wirelessly powering a capsule robot. *IEEE Transactions on Power Electronics*, *39*(1), 1826-1839. https://doi.org/10.1109/TPEL.2023.3321845

[2] Zhang, J., Li, H., Kong, X., Zhou, J., Shi, G., Zang, J., & Wang, J. (2024). A novel multiple-medium-AC-port power electronic transformer. *IEEE Transactions on Industrial Electronics*, *71*(7), 6568-6578. https://doi.org/10.1109/TIE.2023.3301550

[3] Zhang, J., Feng, X., Zhou, J., Zang, J., Wang, J., Shi, G., & Li, Y. (2023). Series-shunt multiport soft normally open points. *IEEE Transactions on Industrial Electronics*, *70*(11), 10811-10821. https://doi.org/10.1109/TIE.2022.3229375

[4] Yao, Y., Shu, F., Cheng, X., Liu, H., Miao, P., & Wu, L. (2023). Automotive radar optimization design in a spectrally crowded V2I communication environment. *IEEE Transactions on Intelligent Transportation Systems*, *24*(8), 8253-8263. https://doi.org/10.1109/TITS.2023.3264507

[5] Li, N., Zhang, C., Liu, Y., Zhuo, C., Liu, M., Yang, J., & Zhang, Y. (2024). Single-degree-of-freedom hybrid modulation strategy and light-load efficiency optimization for dual-active-bridge converter. *IEEE Journal of Emerging and Selected Topics in Power Electronics*, *12*(4), 3936-3947. https://doi.org/10.1109/JESTPE.2024.3396340

[6] Zeng, Z. & Goetz, S. M. (2024). A General Modeling and Analysis of Impacts of Unbalanced Inductance on PWM Schemes for Two-Parallel Interleaved Power Converters. *IEEE Transactions on Power Electronics*, *39*(10), 12235-12248. https://doi.org/10.1109/TPEL.2024.3388024

[7] Huang, S., Sun, C., Wang, R., & Pompili, D. (2025). Toward Adaptive and CoordinatedTransportation Systems: A Multi-Personality Multi-Agent Meta-Reinforcement Learning Framework. *IEEE Transactions on Intelligent Transportation Systems*, 1-14. https://doi.org/10.1109/TITS.2025.3560227

[8] Zeng, Z. & Goetz, S. M. (2024). A General Interchanged Interleaving Carriers for Eliminating DC/Low-Frequency Circulating Currents in Multiparallel Three-Phase Power Converters. *IEEE Transactions on Power Electronics*, *39*(10), 12323-12335. https://doi.org/10.1109/TPEL.2024.3407207

[9] Bendib, B., Belmili, H., & Krim, F. (2015). A survey of the most used MPPT methods: Conventional and advanced algorithms applied for photovoltaic systems. *Renewable and Sustainable Energy Reviews*, *45*, 637-648.

https://doi.org/10.1016/j.rser.2015.02.009
[10] A. Djalab, N. Bessous, M. Rezaoui, & Merzouk, I. (2018). Study of the Effects of Partial Shading on PV Array. *2018 International Conference on Communications and Electrical Engineering (ICCEE)*. https://doi.org/10.1109/CCEE.2018.8634512
[11] Jamal, J., Mansur, I., Rasid, A., Mulyadi, M., Dihyah Marwan, M., & Marwan, M. (2024). Evaluating the shading effect of photovoltaic panels to optimize the performance ratio of a solar power system. *Results in Engineering*, *21*, 101878. https://doi.org/10.1016/j.rineng.2024.101878
[12] He, L., Mo, H., Zhang, Y., Wu, L., & Tang, J. (2025). Adaptive energy management strategy for Extended Range Electric Vehicles under complex road conditions based on RF-IGWO and MGO algorithms. *Energy*, *328*, 136500. https://doi.org/10.1016/j.energy.2025.136500
[13] Alves, T., N. Torres, J. P., Marques Lameirinhas, R. A., & F. Fernandes, C. A. (2021). Different Techniques to Mitigate Partial Shading in Photovoltaic Panels. *Energies*, *14*(13). https://doi.org/10.3390/en14133863
[14] Erol, H. & Uçman, M. (2018). Power optimization in partially shaded photovoltaic systems. *Tehnički glasnik*, *12*(1), 34-38. https://doi.org/10.31803/tg-20180201165044
[15] Chen, X., Cui, J., Liu, Y., Zhang, X., Sun, J., Ai, R., Gu, W., Xu, J., & Lu, H. (2024). Joint Scene Flow Estimation and Moving Object Segmentation on Rotational LiDAR Data. *IEEE Transactions on Intelligent Transportation Systems*, *25*(11), 17733-17743. https://doi.org/10.1109/TITS.2024.3432755
[16] Mirjalili, S., Mirjalili, M., & Yao, X. (2013). Grasshopper optimization algorithm. *IEEE Transactions on Evolutionary Computation*, *17*(1), 18-30. https://doi.org/10.1109/TEVC.2013.2281535
[17] Ali, M., Ahmad, M., Koondhar, M. A., Akram, M. S., Verma, A., & Khan, B. (2023). Maximum power point tracking for grid-connected photovoltaic system using Adaptive Fuzzy Logic Controller. *Computers and Electrical Engineering*, *110*, 108879. https://doi.org/10.1016/j.compeleceng.2023.108879
[18] Yang, Y., Zhang, Z., Zhou, Y., Wang, C., & Zhu, H. (2023). Design of a Simultaneous Information and Power Transfer System Based on a Modulating Feature of Magnetron. *IEEE Transactions on Microwave Theory and Techniques*, *71*(2), 907-915. https://doi.org/10.1109/TMTT.2022.3205612
[19] Ding, F., Zhu, K., Liu, J., Peng, C., Wang, Y., & Lu, J. (2024). Adaptive memory event-triggered output feedback finite-time lane-keeping control for autonomous heavy truck with roll prevention. *IEEE Transactions on Fuzzy Systems*, *32*(12), 6607-6621. https://doi.org/10.1109/TFUZZ.2024.3454344
[20] Wang, S., Cheng, Q., Shangguan, B., Ma, J., Jiao, N., & Liu, T. (2025). Accurate and continuous reactive power control of three-terminal hybrid DC transmission system. *IEEE Transactions on Power Delivery*, *40*(1), 30-40. https://doi.org/10.1109/TPWRD.2024.3480270
[21] Chen, S., Wang, Y., Tian, Z., Xiao, X., Xie, X., & Gomis-Bellmunt, O. (2025). Understanding a type of forced oscillation in grid-forming and grid-following inverter connected systems. *IEEE Transactions on Power Electronics*, *40*(8), 11628-11640. https://doi.org/10.1109/TPEL.2025.3557035
[22] Jiang, M., Zhang, Y., & Zhang, Y. (2022). Multi-Depot Electric Bus Scheduling Considering Operational Constraint and Partial Charging: A Case Study in Shenzhen, China. *Sustainability*, *14*(1), 255. https://doi.org/10.3390/su14010255
[23] Zhang, Y., Zhang, Y., Zheng, B., Cui, H., & Qi, H. (2025). Statistical analysis for estimating the optimized battery capacity for roof-top PV energy system. *Renewable Energy*, *242*, 122491. https://doi.org/10.1016/j.renene.2025.122491
[24] Meng, Q., He, Y., Li, S., Hussain, S., Lu, J., You, G., & Guerrero, J. M. (2025). Adaptive two-step power prediction and improved perturbation method for accelerated MPPT with reduced oscillations in photovoltaic systems. *Energy Reports*, *13*, 5328-5338. https://doi.org/10.1016/j.egyr.2025.04.055
[25] Chang, Y., Ren, Y., Jiang, H., Fu, D., Cai, P., Cui, Z., Li, A., & Yu, H. (2025). Hierarchical adaptive cross-coupled control of traffic signals and vehicle routes in large-scale road network. *Computer-Aided Civil and Infrastructure Engineering*. https://doi.org/10.1111/mice.13508
[26] Asadi, F., Eguchi, K., & Hudgins, J. (2018). *Dynamics and Control of DC-DC Converters*. Morgan & Claypool Publishers. https://doi.org/10.1007/978-3-031-02502-0
[27] Burd, J. T. J., Moore, E. A., Ezzat, H., Kirchain, R., & Roth, R. (2021). Improvements in electric vehicle battery technology influence vehicle lightweighting and material substitution decisions. *Applied Energy*, *283*, 116269. https://doi.org/10.1016/j.apenergy.2020.116269
[28] Chang, W. J., Lee, K. H., Ha, H., Jin, K., Kim, G., Hwang, S. T. et al. (2017). Design Principle and Loss Engineering for Photovoltaic-Electrolysis Cell System. *ACS Omega*, *2*(3), 1009-1018. https://doi.org/10.1021/acsomega.7b00012
[29] Yasa, Y. (2023). A system efficiency improvement of DC fast-chargers in electric vehicle applications: Bypassing second-stage full-bridge DC-DC converter in high-voltage charging levels. *Ain Shams Engineering Journal*, *14*(9), 102391. https://doi.org/10.1016/j.asej.2023.102391
[30] Zuccari, F., Orecchini, F., Santiangeli, A., Suppa, T., Ortenzi, F., Genovese, A., & Pede, G. (2019). Well to wheel analysis and comparison between conventional, hybrid and electric powertrain in real conditions of use. *AIP Conference Proceedings*, *2191*(1), 020158. https://doi.org/10.1063/1.5138891

Contact information:

Nabil MCHIRGUI, **BSc Eng, MSc Eng, and PhD Candidate**
Département d'Informatique et d'Ingénierie, LIMA Research Laboratory,
Université du Québec en Outaouais, 101, rue Saint-Jean-Bosco, Gatineau,
Quebec, Canada J8Y 3G5
E-mail: mchn01@uqo.ca

Ahmed LAKHSSASSI, Ph.D., Eng., Professor, Electronic Engineering
Department of Computer Science and Engineering,
LIMA Laboratory, Université du Québec en Outaouais (UQO),
101, rue Saint-Jean-Bosco, Gatineau, Quebec, Canada J8Y 3G5
E-mail: ahmed.lakhssassi@uqo.ca

Habib KRAIEM, Ph.D., Associate Professor
(Corresponding author)
Center for Scientific Research and Entrepreneurship,
Northern Border University, Arar 73213, Saudi Arabia
E-mail: alhabeeb.kareem@nbu.edu.sa

Mohamed RAHOUTI, Ph.D., Assistant Professor
Department of Computer and Information Science,
Fordham University, 113 W 60th Street, New York, NY 10023, USA
E-mail: mrahouti@fordham.edu

Hady ABDEL MAKSOUD, Ph.D., Assistant Professor
1) Electrical Engineering Department, College of Engineering,
Northern Border University, Arar 1321, Saudi Arabia
2) Electrical Engineering Department, Faculty of Engineering, Menoufia University, Shebin El-Kom 32511, Egypt
E-mail: hady_elgendy@Yahoo.com; hady.elgendy@nbu.edu.sa

Nordine QUADAR, Peng, BSc, MSc, and PhD Candidate
Department of Mathematics and Computer Science,
Royal Military College of Canada, Kingston, ON 11 K7K 7B4, Canada
E-mail: Quadar@rmc.ca